Pergamon

Bioorganic & Medicinal Chemistry, Vol. 5, No. 6, pp 1235–1248, 1997

PII: S0968-0896(97)00038-2
0968-0896/97 $17.00 + 0.00

On the Chemistry of RNA Degradation by Fe·Bleomycin

Chris E. Holmes,[a] Robert J. Duff,[a] Gijs A. van der Marel,[b] Jacques van Boom[b] and Sidney M. Hecht*,[a]

[a]*Departments of Chemistry and Biology, University of Virginia, Charlottesville, Virginia 22901, U.S.A.*
[b]*Department of Organic Chemistry, University of Leiden, Leiden, The Netherlands*

Abstract—The chemistry of RNA degradation by Fe·bleomycin was studied using two RNA substrates that are modified efficiently at a small number of sites by the antitumor antibiotic. Cleavage of a $tRNA^{His}$ precursor transcript by Fe(II)·BLM A_2 was shown to require O_2; cleavage was also observed when the same substrate was treated with Fe(III)·BLM A_2 + H_2O_2. Consistent with earlier observations made for DNA, the extent of $tRNA^{His}$ precursor cleavage was greater for Fe(II)·BLM A_5 than for Fe(II)·BLM A_2; the least cleavage was obtained using Fe(II)·BLM demethyl A_2. By the use of a ^{32}P end labeled $tRNA^{His}$ precursor transcript that was also ^3H labeled within the uracil moieties, it was shown that release of uracil was nearly stoichiometric with tRNA strand scission by Fe(II)·BLM A_2. Nonetheless, treatment of the $tRNA^{His}$ with hydrazine following BLM-mediated cleavage indicated formation of a new product that must have derived from a BLM-induced lesion. Also employed for characterization of BLM cleavage of RNA were the octanucleotides CGCTAGCG, C_3-*ribo*-CGCTAGCG and C_3-*ara*-CGCTAGCG. Analysis of the products of cleavage indicates that Fe·BLM is capable of mediating cleavage by abstraction of a H atom either from C-4′ H or C-1′ H of the chimeric oligonucleotides. © 1997 Elsevier Science Ltd.

Introduction

The bleomycins (BLM's) are a family of antitumor antibiotics originally isolated from *Streptomyces verticillus*.[1] The bleomycins are glycopeptide-derived species of complex structure; the several naturally occurring members of this family generally differ at the C-terminus, as exemplified by the structures of bleomycins A_2, demethyl A_2 and A_5.[2]

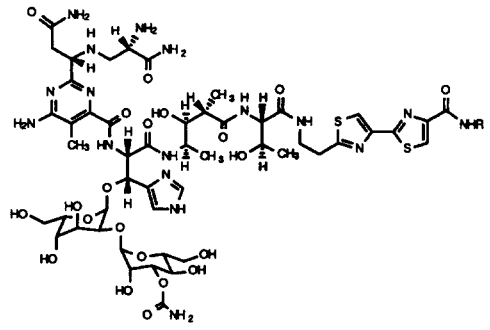

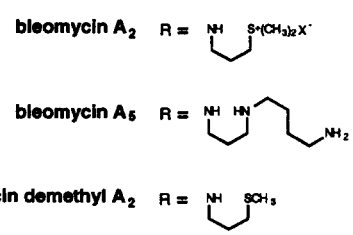

While the antitumor activity of bleomycin has long been thought to involve oxidative degradation of DNA,[3] it has recently been shown in an extensive series of experiments that Fe·BLM can also effect the degradation of RNAs.[4] Although not all RNAs act as substrates for cleavage by bleomycin, RNAs that do act as substrates include several transfer RNAs and tRNA precursor transcripts, as well as messenger RNAs, ribosomal 5S RNA and an RNA–DNA heteroduplex.[5] Degradation of these substrates proceeded efficiently at micromolar concentrations of Fe·BLM and generally resulted in highly selective cleavage. Unlike DNA cleavage, which is generally limited to a subset of the 5′ G-Pyr3′ sequences in DNA,[6] the substrate RNAs also underwent cleavage at other sites, notably those thought to be at the junction between single and double-stranded regions of the RNAs. As a consequence, the sequence selectivity of RNA cleavage is thought to depend not only on RNA primary sequence, but also on RNA conformation.

The chemical transformations mediated by Fe·BLM that result in DNA cleavage have been investigated in detail.[3] DNA degradation is initiated by abstraction of a hydrogen atom from C-4′ of deoxyribose. Under ambient conditions, the major pathway apparently involves reaction of the C-4′ deoxyribose radical with O_2; collapse of the derived C-4′ hydroperoxy intermediate occurs with scission of the C-3′–C-4′ bond of the sugar, affording base propenals and oligonucleotide 3′-phosphoroglycolates in equal amounts.[3] Alternatively, when O_2 concentrations were limiting, the major products were free bases and alkali-labile lesions that arise via a C-4′ OH intermediate. The alkali-labile lesions were shown to be C-4′ hydroxylated apurinic acids.[7]

The chemistry of RNA degradation by bleomycin has been less well characterized than that of DNA.

Presently, we describe the experimental parameters conducive to RNA degradation. It is demonstrated that RNA cleavage is oxidative in nature, requires oxygen and may be potentiated by external reductants such as ascorbate or dithiothreitol. Also shown is the ability to achieve RNA strand scission by admixture of Fe(III)·BLM + H_2O_2. By the use of a tRNA precursor substrate cleaved predominantly at a single position by Fe·BLM and a chimeric DNA oligonucleotide containing a single ribonucleotide at the site of BLM-mediated degradation, we also define and quantify the degradation products. Fe·BLM can abstract either C4′ H or C1′ H from the ribose moiety in (the chimeric) RNAs; cleavage of *B. subtilis* $tRNA^{His}$ precursor with Fe(II)·BLM + O_2 under ambient conditions gave nearly stoichiometric amounts of free uracil and strand breaks, indicating that alkali lable lesions were not major products under the conditions employed.

Results

To further define the chemical nature of the process by which bleomycin mediates RNA degradation, two types of substrates have been employed. The first is an in vitro RNA transcript having the primary sequence of *Bacillus subtilis* $tRNA^{His}$ precursor.[8] This RNA transcript has been shown to undergo efficient cleavage by Fe(II)·BLM A_2, predominantly at uridine$_{35}$ (Fig. 1).[4b] Also employed as a substrate was a self-complementary octanucleotide having the sequence $^{5'}$CGCTAGCG$^{3'}$, as well as two chimeric octanucleotides of the same sequence, but having *ribo*-cytidine or *ara*-cytidine at position 3 (Fig. 1). The DNA octanucleotide, readily accessible in quantity by total synthesis,[9] has been

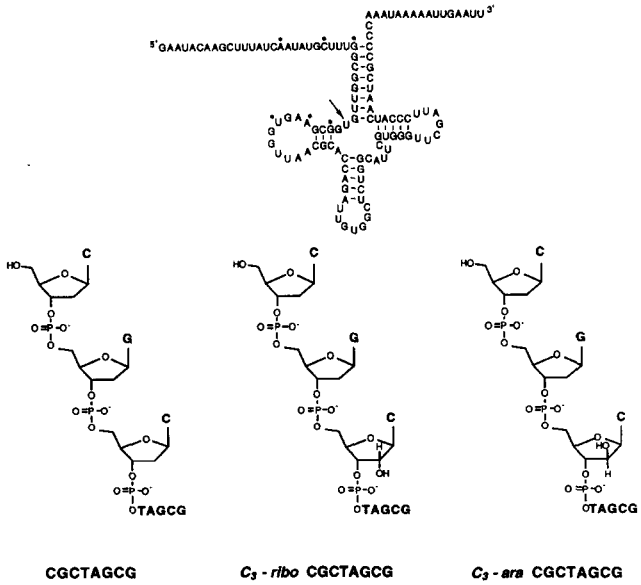

Figure 1. (Top) Cloverleaf representation of the secondary structure of *Bacillus subtilis* tRNAHis precursor showing the major (arrow) and minor (asterisks) sites of Fe·BLM-mediated cleavage. (Bottom) Structure of a DNA octanucleotide cleaved efficiently by Fe·BLM and two chimeric oligonucleotides of similar structure having modified nucleosides at one of the major cleavage sites.

shown to undergo Fe·BLM-mediated oxidative modification at C_3 and C_7. The products formed by oxidation at C_3 are amenable to facile chemical analysis by comparison with authentic synthetic standards.[7a,c,10] Accordingly, the chimeric oligonucleotides were prepared in the belief that they would facilitate definition of the way in which *ribo* and *ara*-nucleotides underwent oxidative degradation.

Bleomycin-mediated degradation of $tRNA^{His}$ precursor

One facet of RNA degradation by Fe(II)·BLM that has not been explored is the ability of individual bleomycin congeners to mediate degradation of an RNA substrate. Virtually all of the studies reported to date have employed BLM A_2, or else the clinically used mixture of bleomycins. As shown in Figure 2, $tRNA^{His}$ precursor was treated with Fe(II)·BLM demethyl A_2, Fe(II)·BLM A_2 and Fe(II)·BLM A_5. All three analogues produced cleavage at U_{35}, the previously identified major cleavage site for Fe(II)·BLM A_2. While the minor cleavage sites observed for BLM A_2 were also produced by Fe(II)·BLM A_5, additional minor cleavage sites near

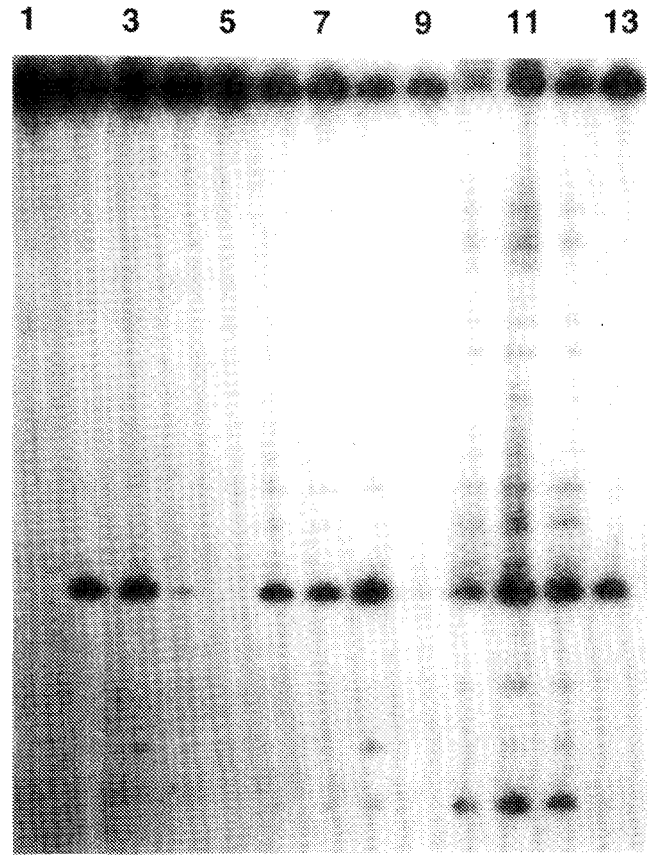

Figure 2. Cleavage of $tRNA^{His}$ precursor by Fe(II)·BLM congeners. Samples of 5′-^{32}P end labeled $tRNA^{His}$ precursor (~3 μM final nucleotide concentration) were treated with each of three BLM congeners at four different concentrations in the presence of Fe^{2+}. Lane 1, $tRNA^{His}$ precursor alone; lanes 2–5, Fe(II)·BLM demethyl A_2 at concentrations of 200, 100, 10 and 2 μM, respectively; lanes 6–9, Fe(II)·BLM A_2 at concentration of 200, 100, 10, and 2 μM, respectively; lanes 10–13, Fe(II)·BLM A_5 at concentrations of 200, 100, 10, and 2 μM, respectively.

the 3′-end of the tRNA precursor were also observed in the latter reaction. Treatment with Fe(II)·BLM demethyl A_2 resulted in cleavage essentially exclusively at U_{35}.

Differences in the overall facility of cleavage were also seen with the order of potency being BLM A_5 > BLM A_2 > BLM demethyl A_2. Fe(II)·BLM demethyl A_2-mediated cleavage of $tRNA^{His}$ precursor was seen only at 250 μM and 100 μM concentrations, while cleavage was observed at 250 μM, 100 μM and 10 μM Fe(II)·BLM A_2 concentrations. Fe(II)·BLM A_5 produced cleavage at concentrations as low as 1 μM. The increased cleavage potential of BLM A_2 and BLM A_5 was reflected in increased conversion to the major product derived from U_{35}, as well as enhancement of minor cleavage sites. A quantitative analysis indicated that while BLM demethyl A_2 produced approximately 10% conversion to major and minor products, up to 70% conversion was obtained with Fe(II)·BLM A_5. The order of potencies of the three BLMs presumably reflects the number of positively charged groups at the C-terminus of these congeners; analogous effects have been noted previously for DNA cleavage[11] and for the binding of substituted bithiazoles to DNA substrates.[12] The ostensible lack of cleavage of $tRNA^{His}$ precursor at sites other than U_{35} by Fe(II)·BLM demethyl A_2 presumably reflects the diminished potency of this analogue relative to BLM A_2 and BLM A_5, rather than any fundamental difference in their modes of substrate recognition.

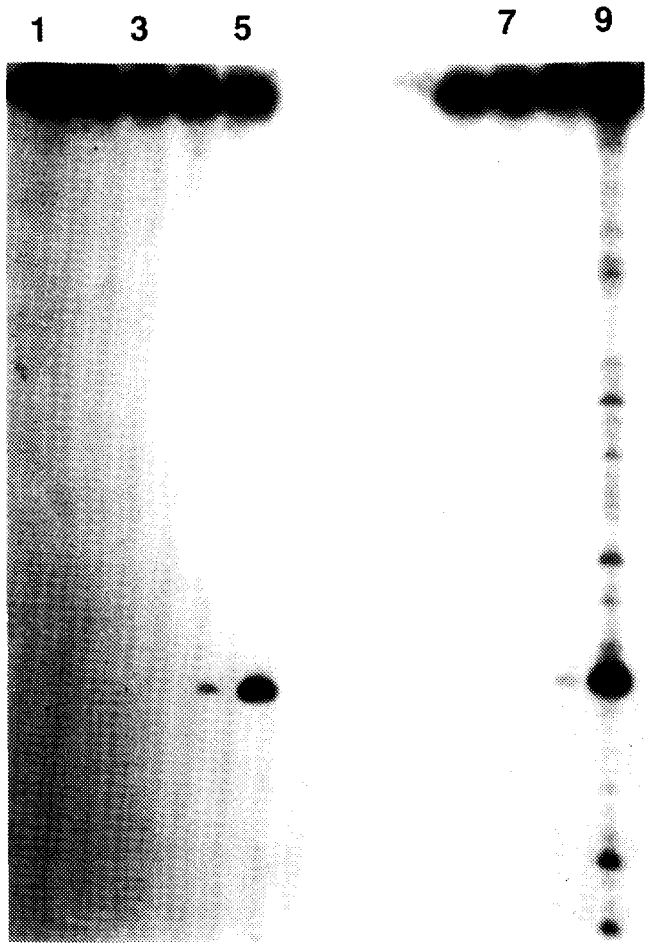

Figure 3. Oxygen dependence of the cleavage of $tRNA^{His}$ precursor by Fe(II)·BLM. Samples of 5′-^{32}P end labeled $tRNA^{His}$ precursor (~3 μM final nucleotide concentration) were treated with BLM A_2 at 3–4 ppm oxygen concentration (lanes 1–4) or under ambient conditions (lanes 5–7). Lane 1, $tRNA^{His}$ precursor alone; lane 2, 10 μM BLM A_2; lane 3, 10 μM Fe^{2+}; lane 4, 10 μM Fe(II)·BLM A_2; lane 5, 10 μM Fe(II)·BLM A_2; lane 6, $tRNA^{His}$ precursor alone; lane 7, 10 μM Fe^{2+}. Lanes 8 and 9 contained 100 μM Fe(II)·BLM A_2 and were run under reduced oxygen and ambient conditions, respectively.

Also explored was the need for oxygen in Fe(II)·BLM-mediated degradation of RNA. Oxygen or an oxygen surrogate is required for the formation of activated BLM in Fe(II)·BLM-mediated cleavage of DNA. Additionally, O_2 has been proposed to combine with the initially formed C4′ deoxyribose radical, leading to one set of DNA degradation products that includes base propenals. The requirement for formation of an activated species from Fe·BLM for RNA cleavage was first suggested by treatment of $tRNA^{His}$ precursor with Fe(II)·BLM or Fe(III)·BLM. RNA cleavage proceeded readily in the presence of Fe(II)·BLM under ambient conditions, but Fe(III)·BLM did not support efficient substrate degradation.[4b]

As shown in Figure 3, degradation of $tRNA^{His}$ precursor under reduced oxygen tension (3–4 ppm) resulted in a dramatic reduction in cleavage as compared to cleavage obtained under ambient conditions. This reduction was particularly evident at 100 μM Fe(II)·BLM concentration. The minimal cleavage observed at low oxygen tension was limited to the U_{35} cleavage site; it is presumed to have resulted from the residual oxygen present.

The degradation of DNA is believed to be mediated by an 'activated BLM' complex consisting of BLM, oxygen and a redox active metal.[3,13] Burger et al.[14] demonstrated that this activated species can be produced by reductive activation in the presence of Fe^{2+} + O_2 or else by admixture of Fe^{3+} + H_2O_2. Therefore, the ability of Fe(III)·BLM + H_2O_2 to form activated BLM capable of supporting the cleavage of $tRNA^{His}$ precursor was also investigated (Fig. 4). Cleavage of the $tRNA^{His}$ precursor substrate was effected in the presence of 100 μM Fe(III)·BLM + 1 mM H_2O_2. Interestingly, activation of Fe(III)·BLM by hydrogen peroxide resulted in significantly more cleavage of the RNA substrate than that produced by a comparable concentration of Fe(II)·BLM A_2 + O_2 (cf lanes 5 and 6). This enhancement in cleavage was also evident at 10 μM Fe·BLM concentration (data not shown). While both activation methods resulted in cleavage of $tRNA^{His}$ precursor at U_{35} (the major site of strand scission) and several minor sites, at least two minor cleavage sites appeared to depend on the method employed for BLM activation (Fig. 4). A minor cleavage site near the 3′-end of the $tRNA^{His}$ precursor was observed in Fe(III)·BLM A_2 + H_2O_2 reactions, but was clearly not present in reactions mediated by Fe(II)·BLM +O_2. In addition, a

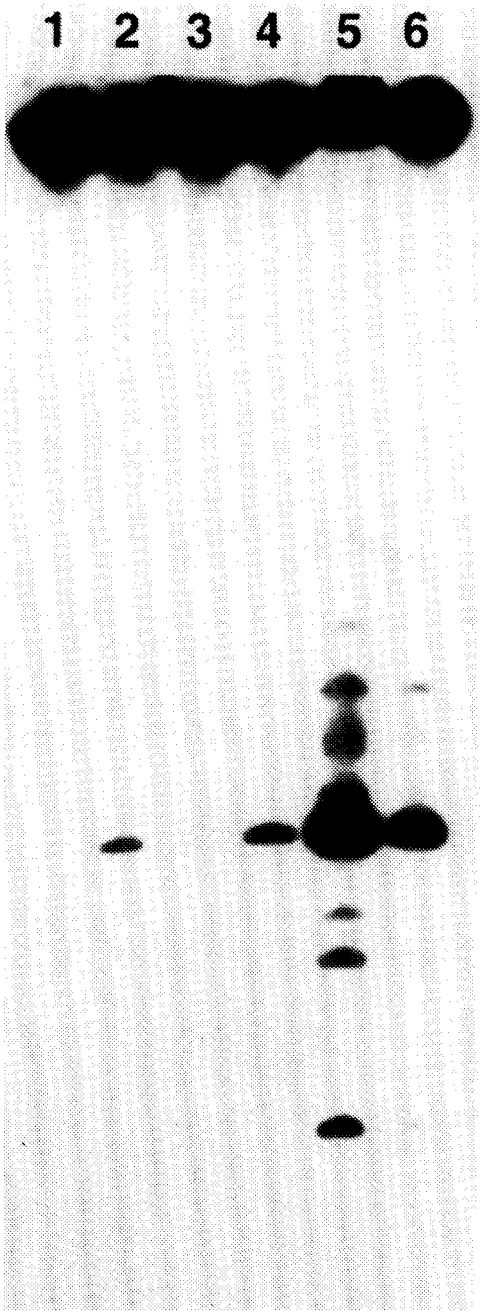

Figure 4. Cleavage of $tRNA^{His}$ precursor in the presence of Fe(III)·BLM A_2 + H_2O_2. Samples of 5′-^{32}P end labeled $tRNA^{His}$ precursor (~3 μM final nucleotide concentration) were treated with BLM that had been activated under different conditions. Lane 1, $tRNA^{His}$ precursor alone; lane 2, 100 μM BLM A_2 + 1 mM H_2O_2; lane 3, 100 μM Fe^{3+} + 1 mM H_2O_2; lane 4, 100 μM Fe(III)·BLM A_2; lane 5, 100 μM Fe(III)·BLM A_2 + 1 mM H_2O_2; lane 6, 100 μM Fe(II)·BLM A_2. The cleavage observed in lanes 2 and 4 is attributed to adventitious metal ions.

minor product band present near the 5′-end of $tRNA^{His}$ precursor in the Fe(II)·BLM A_2 + O_2 reactions was not observed when cleavage was produced by Fe(III)·BLM + H_2O_2.

BLM-mediated cleavage of numerous RNA substrates has been demonstrated using Fe(II)·BLM + O_2 for activation.[4] Under these conditions, the formation of activated BLM is known to require an additional electron.[15] In DNA degradation reactions, this electron may be supplied by exogenous reducing agents such as 2-mercaptoethanol, dithiothreitol and ascorbate.[10] In the absence of such reductants, it is believed that the electron is obtained from the collision of oxygenated Fe(II)·BLM with a second Fe(II)·BLM, affording one activated Fe·BLM and Fe(III)·BLM.[15]

Table 1. Effect of ascorbate on the cleavage of $tRNA^{His}$ precursor by Fe(II)·BLM A_2

BLM A_2 (μM)	Fe^{2+} (μM)	Na ascorbate (mM)	Cleavage of $tRNA^{His}$ precursor (% conversion)
—	—	—	0
25	—	2	12
—	25	2	1
25	25	—	19
25	25	0.5	69
25	25	2	77

In contrast to DNA, the ability of external reductants to potentiate the cleavage of RNA by Fe(II)·BLM + O_2 has not been reported. As shown in Table 1, the addition of 2 mM ascorbate to a cleavage reaction containing 25 μM Fe(II)·BLM A_2 and $tRNA^{His}$ precursor resulted in significantly increased cleavage of the RNA substrate; cleavage at both major and minor sites was increased (data not shown). Lower ascorbate concentrations (500 μM and 1 mM) also resulted in a substantial increase in substrate cleavage. The potentiation of RNA cleavage reactions by the addition of dithiothreitol has also been demonstrated for the $tRNA^{His}$ precursor as well as yeast $tRNA^{Asp}$ (data not shown).

Characterization of RNA degradation products

Fe(II)·BLM-mediated cleavage of $tRNA^{His}$ precursor occurs efficiently at one major site, $uridine_{35}$.[4b,c] To permit direct analysis of the product(s) resulting from cleavage at this site, a $tRNA^{His}$ precursor substrate incorporating both ^{32}P and ^{3}H radiolabels was employed. The precursor $tRNA^{His}$ molecule was transcribed from a linearized plasmid in the presence of [α-^{32}P]CTP and [5,6-^{3}H]UTP to produce an intact substrate ^{32}P-labeled in the ribose phosphate backbone as well as ^{3}H-labeled in the base moiety of incorporated uridines. The resulting substrate was treated with Fe(II)·BLM; aliquots of the reaction mixture were analyzed both by denaturing polyacrylamide gel electrophoresis as well as HPLC.

The HPLC profile of eluted radioactivity following treatment of 8.5 μM $tRNA^{His}$ precursor (final nucleotide concentration) with 250 μM Fe(II)·BLM is shown in Figure 5. An authentic uracil standard co-eluted with the major peak of radioactivity at 6.7 min under the conditions of this experiment. Polyacrylamide gel analysis confirmed cleavage of the substrate at one

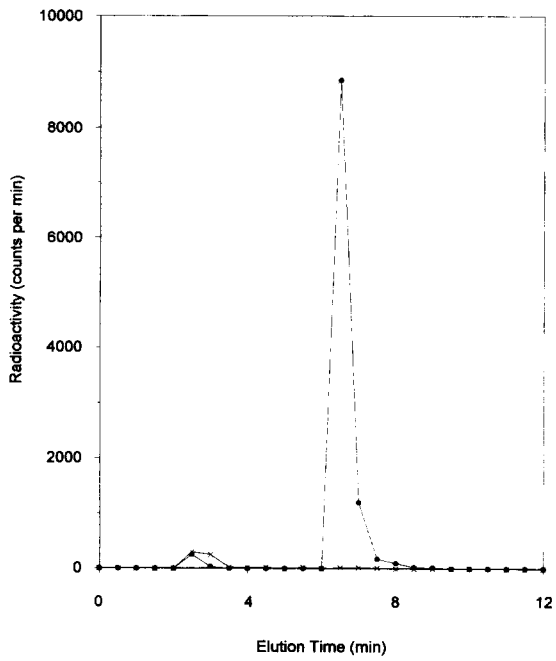

Figure 5. HPLC elution profile of products formed from [^{3}H]uracil-labeled tRNA^{His} precursor upon treatment with Fe(II)·BLM. Samples of tRNA^{His} precursor prepared by transcription in the presence of [5,6-^{3}H]UTP and [α-^{32}P]CTP were subjected to treatment with Fe(II)·BLM A_2 and then analyzed in parallel by HPLC and PAGE. Treatment with 250 μM Fe(II)·BLM A_2 gave a single major peak of radiolabeled material at about 6.7 min that co-eluted with authentic uracil (●). Essentially all ^{3}H-labeled material eluted with the authentic standard. No [^{3}H]uracil was observed when the tRNA^{His} precursor transcript was treated with 250 μM BLM A_2 (×) or analyzed without any treatment (not shown).

major site (data not shown). While the method used for the incorporation of a ^{32}P label precluded sequencing, the presumed site of cleavage was U_{35}. Quantification of this cleavage band on the polyacrylamide gel revealed approximately 13% cleavage of the tRNA^{His} precursor at U_{35}; this corresponded to 4.7 picomoles of strand breaks at U_{35}. Parallel HPLC quantification of free uracil release indicated the production of 3.9 picomoles of uracil, i.e. an essentially stoichiometric relationship between strand scission and uracil release. In replicate experiments, the measured extent of uracil release never exceeded the calculated number of strand breaks at U_{35}, suggesting the absence of large numbers of lesions in which base release had occurred without concomitant strand scission.

Fe·BLM-mediated DNA degradation affords two sets of products, only one of which leads directly to strand scission. The other set of products includes free bases and an alkali labile lesion; treatment with base effects cleavage of the alkali labile product. Additionally, oxidative cleavage initiated at C-1′ of a chimeric DNA oligonucleotide containing a single ribonucleotide has been documented; the initially formed products included a free base, but no strand scission products.[16] Accordingly, we attempted to determine whether Fe(II)·BLM treatment of tRNA^{His} precursor afforded

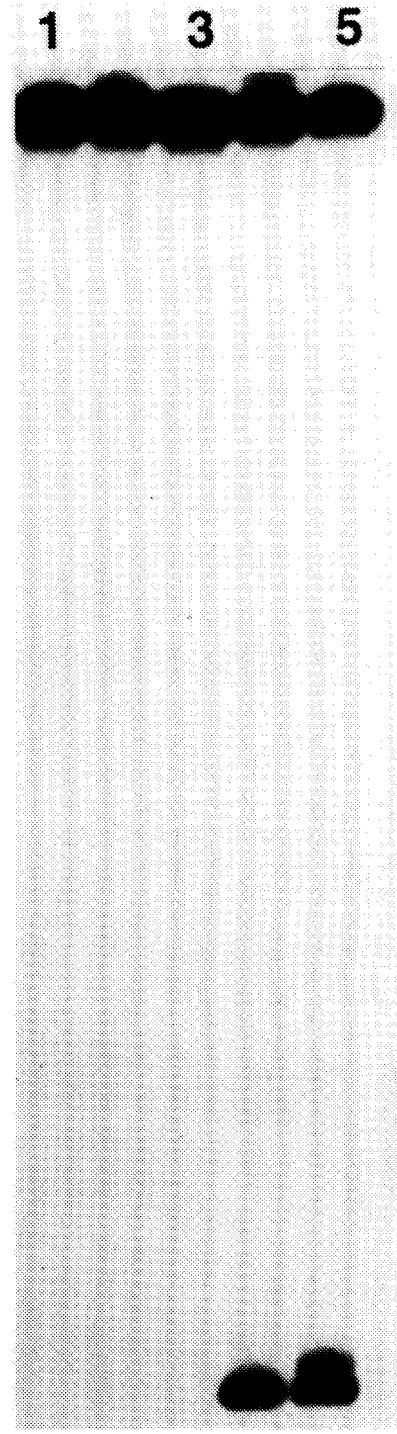

Figure 6. Effects of hydrazine and alkali on Fe(II)·BLM-treated tRNA^{His} precursor. Samples of 5′-^{32}P end labeled tRNA^{His} precursor (~1 μM final nucleotide concentration) were treated with Fe·BLM and either hydrazine or alkali. Lane 1, tRNA^{His} precursor alone; lane 2, 200 μM BLM A_2, then 50 mM NH_2NH_2; lane 3, 200 μM Fe^{2+}, then 50 mM NH_2NH_2; lane 4, 200 μM Fe(II)·BLM A_2; lane 5, 200 μM Fe(II)·BLM A_2, then 50 mM NH_2NH_2.

lesions that did not lead directly to strand scission products.

As anticipated on the basis of the inherent chemical lability of RNA, NaOH treatment of Fe·BLM cleavage reaction containing 5′-^{32}P end labeled tRNA^{His} pre-

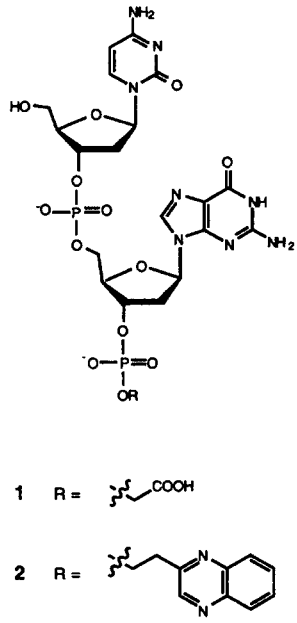

Figure 7. Modified dinucleotides prepared for analysis of Fe·BLM-mediated octanucleotide degradation.

cursor resulted in complete degradation of the substrate (not shown). While careful titration of the amount of alkali employed might have permitted selective unmasking of the putative alkali labile lesion, we chose instead to employ hydrazine, which has been used to convert the alkali labile lesion derived from DNA to a pyridazine derivative.[7c] Treatment of $tRNA^{His}$ precursor successively with Fe(II)·BLM and then with hydrazine produced an additional, slower migrating band at the major U_{35} cleavage site (Fig. 6, cf lanes 4 and 5). This observation provided strong inferential evidence that some lesion not leading to RNA strand scission directly actually was formed as a consequence of Fe(II)·BLM treatment of the $tRNA^{His}$ precursor.

Bleomycin-mediated degradation of chimeric octanucleotides

The chemical products of Fe·BLM-mediated DNA cleavage have been characterized previously using the DNA dodeconucleotide $CGCT_3A_3GCG$, which undergoes modification almost exclusively at C_3 and C_{11}.[10] Subsequently, the structurally simpler octanucleotide CGCTAGCG has been shown to afford the analogous products of oxidation at C_3 and C_7.[15b] In both cases, the strategy employed for product characterization involved HPLC quantification of reaction products in comparison with authentic synthetic standards.

To further characterize the products of Fe(II)·BLM-mediated RNA cleavage, we have used chimeric octanucleotides as substrates for Fe(II)·BLM one of which contains *ribo*-cytidine at position 3 and the other *ara*-cytidine at this position (Fig. 1). In order to characterize the possible products whose formation could be anticipated in analogy with the known chemistry of Fe·BLM-mediated oligonucleotide degradation, two modified dinucleotides of the forms CpGpx were prepared (Fig. 7). The synthesis of dinucleotide **1** has been described previously;[17] the synthetic scheme

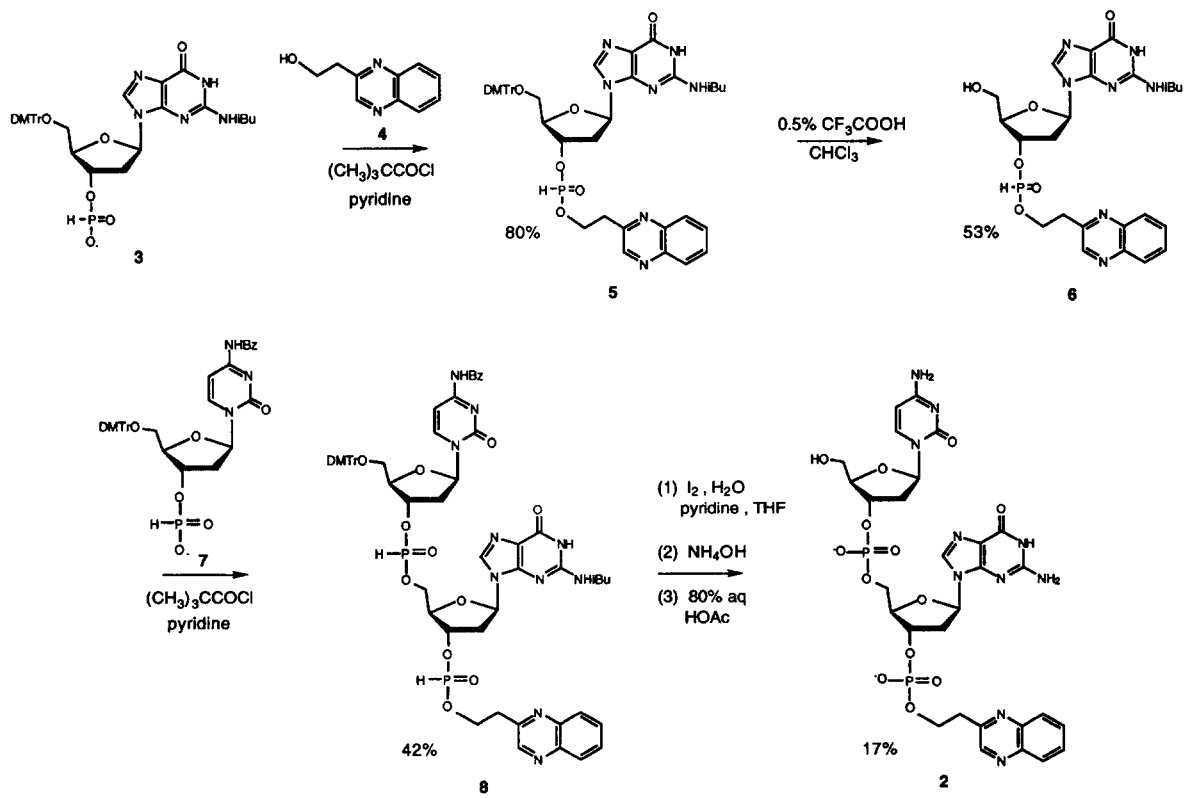

Scheme 1. Synthesis of the quinoxaline derivative of CpG (2).

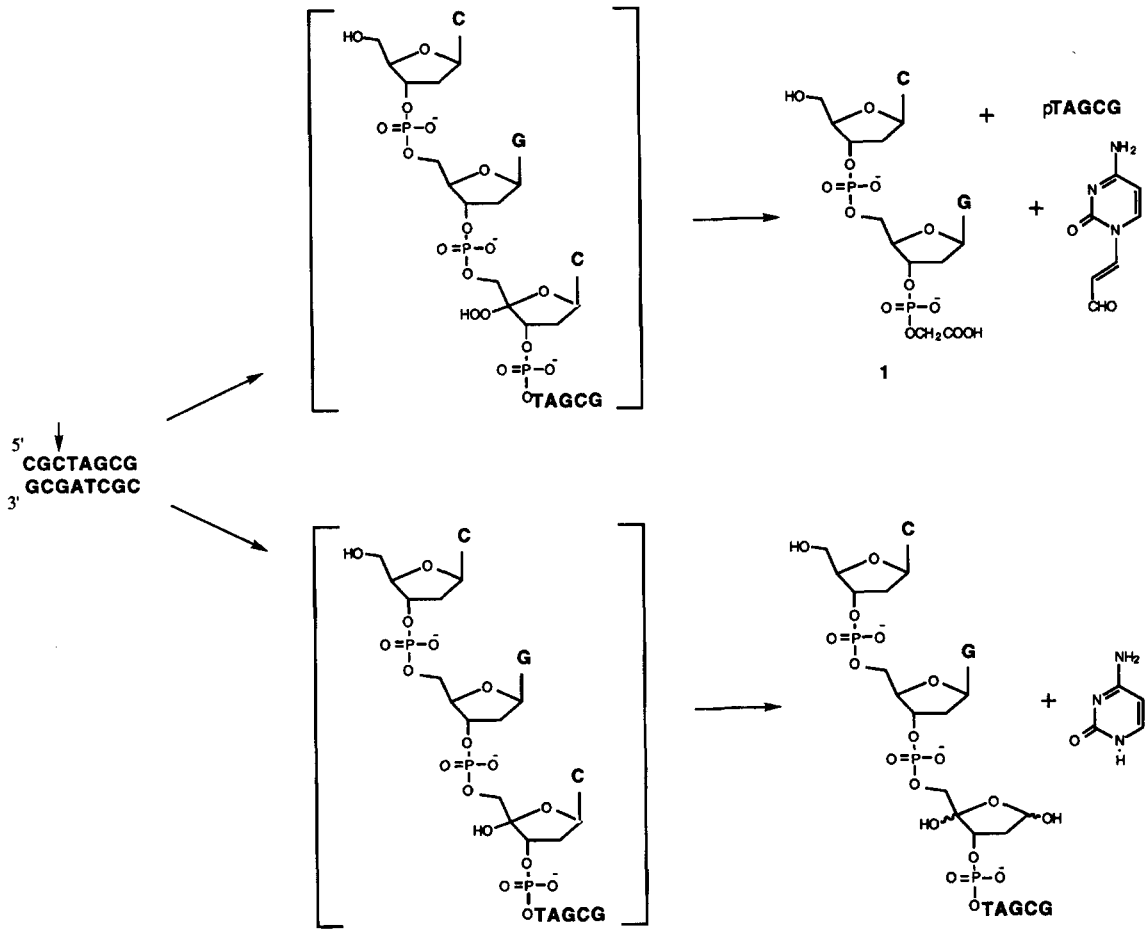

Scheme 2. Products resulting from the degradation of CGCTAGCG at cytidine$_3$ by Fe(II)·BLM.

employed for the elaboration of **2** is outlined in Scheme 1.

As shown in Scheme 1, 2′-(2-hydroxyethyl)quinoxaline (**4**) was condensed with a suitably protected 2′-deoxyguanosine-3′-H-phosphonate derivative (**3**) via the agency of pivaloyl chloride. The resulting deoxyguanosine derivative (**5**) was detritylated to afford **6** and then condensed with a protected 2′-deoxycytidine-3′-H-phosphonate (**7**). The fully protected H-phosphonate **8** that resulted from the condensation was then oxidized with aqueous iodine and deblocked. Dinucleotide **2**, bearing a hydroxyethylquinoxaline moiety, was purified by C_{18} reverse phase HPLC. Although the final deblocking steps proceeded in low overall yield, they were nonetheless superior to alternative routes in which deblocking involved phosphotriester intermediates attached to the quinoxaline moiety. The latter species were prone to facile extrusion of vinylquinoxaline, which must form by a β-elimination mechanism.

BLM-mediated DNA degradation products obtained using the octanucleotide d(CGCTAGCG) have supported DNA degradation pathways involving initially formed C4′-hydroperoxy and C4′-hydroxy intermediates (Scheme 2).[3] As shown, the C4′-hydroperoxy intermediate affords equimolar amounts of $CpGp_{CH_2COOH}$ (**1**) cystosine propenal and pTAGCG when formed at C_3; all of these were actually observed (Table 2). An analogous set of products is formed when

Table 2. Products resulting from treatment of octanucleotide substrates with Fe(II)·BLM A_2

	Products (μM)					
CGCTAGCG	Cytosine	Cytosine propenal	$CpGp_{CH_2COOH}$ (1)	CpGp derivative 2[a]	5′-dGMP	Total lesions[b]
Deoxy	43	77	15	0	62	120
C_3-*ribo*	69	51	9	~1	59	120
C_3-*ara*	59	55	29	40	30	114

[a]Formed upon additional treatment with 1,2-diaminobenzene.
[b]Calculated as the total of cytosine + cytosine propenal.

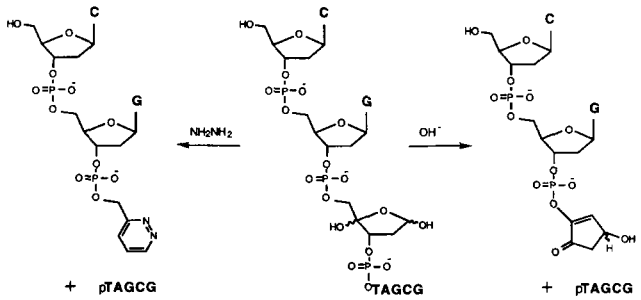

Scheme 3. Products resulting from degradation of the Fe·BLM-induced alkali-labile lesion with base and hydrazine.

oxidative cleavage obtains at C_7.[10,15b] The total amount of strand scission products is defined by the amount of cytosine propenal formed (77 μM in Table 2). The extent of cleavage at C_3 and C_7 can be determined from the amounts of $CpGp_{CH_2COOH}$ (15 μM) and 5′-GMP (62 μM), respectively.[10,15b]

The quantitation of products resulting from the initially formed C4′-hydroxy intermediate can be carried out in similar fashion. The total of all such products is equal to the total amount of free base formed (43 μM in Table 2).[7a,c] The extent of modification at positions C_3 and C_7 can be determined most conveniently after cleavage of the formed alkali labile lesions with a reagent such as a base or hydrazine (Scheme 3).

Analysis of the products resulting from the cleavage of the *ara*- and *ribo*-cytidine-containing octanucleotides indicated the production of cytosine, cytosine propenal, $CpGp_{CH_2COOH}$ (**1**) and 5′-GMP (Table 2). In analogy to octadeoxynucleotide cleavage, the production of $CpGp_{CH_2COOH}$ (**1**) strongly suggests cleavage at the cytidine$_3$ via a C4′-hydroperoxy intermediate. While cytosine propenal and 5′-GMP were presumably formed from analogous cleavage at cytidine$_7$, no hydroxylated cytosine propenal was detected concomitant with cleavage at C_3. This observation was not surprising since it is expected that the hydroxylated propenal would readily hydrolyze to afford 2-hydroxymalondialdehyde and cytosine. In fact, both C_3-*ribo*-CGCTAGCG and C_3-*ara*-CGCTAGCG afforded increased amounts of cytosine relative to CGCTAGCG when treated with Fe(II)·BLM.[18] *N*-Methylguanidine was employed in an effort to trap putative 2-hydroxymalondialdehyde as 5-hydroxy-2-methylaminopyrimidine,[19] but the formation of this species could not be detected even when an authentic sample was employed to assure that the time of elution from HPLC columns was known.

The formation of $CpGp_{CH_2COOH}$ (**1**) was further confirmed by polyacrylamide gel electrophoretic analysis of the reaction mixture employing C_3-*ara*-CGCTAGCG as a substrate. As seen in Figure 8, treatment of C_3-*ara*-CGCTAGCG with Fe(II)·BLM A_2 produced a band that co-migrated with authentic (5′-^{32}P end labeled) $CpGp_{CH_2COOH}$ (cf lanes 2–5). These results support the interpretation that the faster migrating band formed upon treatment of 5′-^{32}P end labeled $tRNA^{His}$ precursor

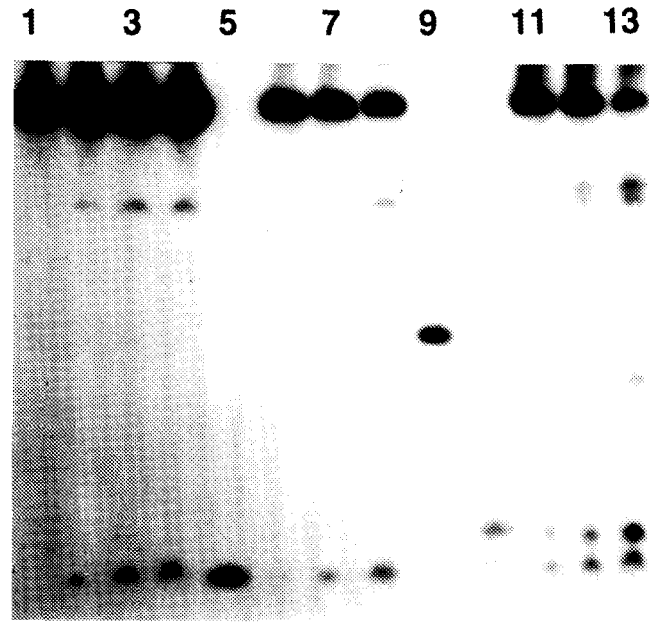

Figure 8. Effects of diaminobenzene and hydrazine on Fe(II)·BLM-treated C_3-*ara*-CGCTAGCG. Samples of 5′-^{32}P end labeled C_3-*ara*-CGCTAGCG (6.25 μM final octanucleotide concentration) were treated with Fe·BLM and either 1,2-diaminobenzene or hydrazine. Lane 1, 5′-^{32}P end labeled C_3-*ara*-CGCTAGCG alone; lane 2, 50 μM BLM A_2 + 100 μM Fe^{2+}; lane 3, 100 μM BLM A_2 + 200 μM Fe^{2+}; lane 4, 200 μM BLM A_2 + 400 μM Fe^{2+}; lane 5, authentic 5′-^{32}P end labeled $CpGp_{CH_2COOH}$; lane 6, 50 μM BLM A_2 + 100 μM Fe^{2+},then 250 mM 1,2-diaminobenzene; lane 7, 100 μM BLM A_2 + 200 μM Fe^{2+}, then 250 mM 1,2-diaminobenzene; lane 8, 200 μM BLM A_2 + 400 μM Fe^{2+}, then 250 mM 1,2-diaminobenzene; lane 9, authentic 5′-^{32}P end labeled CpGp derivative **2**; lane 10, authentic 5′-^{32}P end labeled CpGp; lane 11, 50 μM BLM A_2 + 100 μM Fe^{2+}, then 250 mM NH_2NH_2; lane 12, 100 μM BLM A_2 + 200 μM Fe^{2+}, then 250 mM NH_2NH_2; lane 13, 200 μM BLM A_2 + 400 μM Fe^{2+}, then 250 mM NH_2NH_2. Although not readily apparent in the photograph, the original gel clearly showed bands in lanes 6–8 that co-migrated with authentic quinoxaline derivative **2**. Densitometric analysis indicated that these had intensities 0.2, 3.2 and 6.6%, respectively, that of the band in lane 9.

with Fe(II)·BLM was the oligonucleotide 3′-phosphoroglycolate product (Fig. 6, lane 5).

As noted above, Fe·BLM-mediated DNA degradation also proceeds via a second pathway involving an alkali labile intermediate and the formation of a free base. The alkali labile intermediate formed from DNA by treatment with Fe·BLM can be converted readily to a pyridazine derivative by treatment with hydrazine[7c] (Scheme 3). That an analogous transformation can be obtained for an RNA-derived alkali labile lesion was suggested by the observation of a new band arising on a polyacrylamide gel of a 5′-^{32}P end labeled sample of $tRNA^{His}$ precursor treated with NH_2NH_2 after initial incubation with Fe(II)·BLM (Fig. 6, lane 5).

Treatment of the C_3-*ara*- and C_3-*ribo*-substituted octanucleotides with Fe(II)·BLM, and subsequently with hydrazine, resulted in the formation of a few new products, one of which had a mobility entirely consistent with that expected for the hydroxylated pyridazine derivative, (Fig. 8; cf Scheme 3). However,

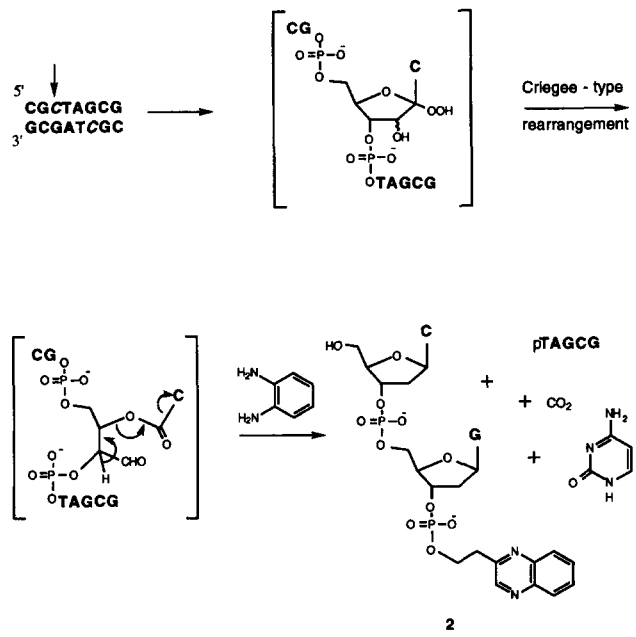

Scheme 4. Formation of the quinoxaline derivative of CpGp (**2**) by successive treatments of C_3-*ribo* and C_3-*ara*-CGCTAGCG with Fe(II)·BLM and 1,2-diaminobenzene.

in the absence of an authentic synthetic standard, the identity of this new product is uncertain.

Also formed during hydrazine treatment of (5′-^{32}P end labeled) C_3-*ara*-CGCTAGCG that had previously been incubated in the presence of Fe(II)·BLM A_2 was a product that co-migrated with authentic (5′-^{32}P end labeled) CpGp. Earlier studies with DNA-derived alkali lesions demonstrated that these could be converted to oligonucleotide 3′-phosphates efficiently under appropriate basic conditions.[7c] The present observation seems entirely consistent, and further extends the analogy between the chemistry of DNA and RNA degradation by Fe(II)·BLM.

One way in which the chemistry of DNA and RNA cleavage may not be analogous involves participation of C1′ H in BLM-mediated oxidative transformations. Studies of DNA degradation by Fe(II)·BLM have failed to provide any evidence for C1′ H abstraction. In contrast, both C_3-*ribo*-CGCTAGCG and C_3-*ara*-CGCTAGCG have previously been shown to afford the quinoxaline derivative of CpGp (**2**) when treated successively with Fe(II)·BLM and 1,2-diaminobenzene.[16] The formation of dinucleotide **2** can be envisioned as shown in Scheme 4.

The formation of this derivative of CpGp was also apparent in the octanucleotide degradation experiments carried out in the present study (Table 2). Consistent with earlier experience, oxidative transformation involving abstraction of C1′ H represented about 10% of all lesions formed at ribocytidine$_3$ of C_3-*ribo*-CGCTAGCG and about 60% of all lesions formed from the *ara*-cytidine moiety in C_3-*ara*-CGCTAGCG by treatment with Fe(II)·BLM A_2. Further quantification of dinucleotide **2** was obtained by the use of [^{14}C]1,2-diaminobenzene. As shown in Table 3, there was very good correspondence between the extent of dinucleotide quinoxaline derivative (**2**) formation estimated by the radioactivity and ultraviolet absorption of the sample formed from C_3-*ara*-CGCTAGCG. Additional evidence for the formation of quinoxaline derivative **2** was also obtained from analysis of polyacrylamide gels. As shown in Figure 8, treatment of (5′-^{32}P end labeled) C_3-*ara* CGCTAGCG with Fe(II)·BLM, and subsequently with 1,2-diaminobenzene, resulted in the formation of a product band which comigrated with (5′-^{32}P end labeled) dinucleotide quinoxaline derivative **2**. In a similar experiment, unlabeled C_3-*ara*-CGCTAGCG was treated with Fe(II)·BLM A_2 and 1,2-diaminobenzene and subsequently subjected to HPLC analysis. The eluate was monitored at 260 and

Table 3. Quantification of dinucleotide **2** formed by successive treatments of C_3-*ara*-CGCTAGCG with Fe(II)·BLM and 1,2-diaminobenzene

Assay method	Dinucleotide **2** (μM)
A_{320}[a]	38–42
Specific activity[b]	40

[a]Molar absorptivity determined using an authentic synthetic sample. [b]Based on the known specific activity of [^{14}C]1,2-diaminobenzene employed in the assay.

Figure 9. Analysis of product resulting from treatment of C_3-*ara*-CGCTAGCG with Fe·BLM, then 1,2-diaminobenzene. A sample of C_3-*ara*-CGCTAGCG (250 μM final octanucleotide concentration) was treated with 400 μM BLM A_2 + 800 μM Fe^{2+}, then with 500 mM 1,2-diaminobenzene. Putative CpGp derivative **2** was isolated by C_{18} reverse-phase HPLC, then 5′-^{32}P end labeled and analyzed by 20% deaturing PAGE. Lane 1, authentic 5′-^{32}P end labeled CpGp derivative **2** alone; lane 2, putative quinoxaline derivative of CpGp (**2**), isolated by HPLC following degradation of C_3-*ara*-CGCTAGCG and then 5′-^{32}P end labeled; lane 3,5′-^{32}P end labeled C_3-*ara*-CGCTAGCG alone.

320 nm; a peak at 33.9 min co-eluted with the authentic quinoxaline derivative of CpGp (**2**). This fraction was collected and the product was subsequently 5-^{32}P end labeled using T4 polynucleotide kinase + [γ-^{32}P]ATP. As shown in Figure 9, this material also co-migrated with the authentic (5′-^{32}P end labeled) quinoxaline derivative of CpGp.

Discussion

Although the ability of Fe(II)·BLM to effect the strand scission of all major classes of RNAs has been well established,[4,5] and numerous examples of substrate molecules have been described, relatively little is known about the actual chemical events involved. Presently, we have shown using tRNA^{His} precursor as a substrate that the potency of RNA strand scission was in direct proportion to the number of positively charged functional groups at the C-terminus of bleomycin. Thus BLM A_5, bearing two positive charges within the spermidine C-substituent, cleaved the tRNA^{His} precursor substrate with much greater efficiency than BLM A_2 which has only a single positive charge within its analogous C-substituent (Fig. 2). BLM demethyl A_2, which lacks any positive charge at the C-terminus, cleaved the RNA substrate with the least efficiency. These findings are not only parallel to the relative potencies of these analogues in DNA degradation[11] and unwinding;[20] they are also consistent with the DNA binding capabilities of bithiazole analogues bearing the same C-substituents.[12]

A related issue not addressed directly in this study is the quantitative relationship between DNA and RNA binding by BLM and the extent of cleavage of these biopolymers. In an earlier study,[21] it was established that a 'tDNA' was degraded with greater facility than the corresponding tRNA transcript in spite of the fact that the tRNA was bound more avidly by Fe·BLM. This observation argues that the relationship between polynucleotide binding and cleavage by BLM is not straightforward; nonetheless quantitative definition of the relationship between binding and cleavage at single sites remains an important goal.

Also investigated in some detail were the parameters conducive to Fe·BLM activation for RNA degradation. As shown in Figure 3, RNA strand scission of the *B. subtilis* tRNA^{His} substrate obtained only when oxygen was present, an observation made previously for DNA strand scission.[22] Also analogous to the chemistry of DNA[3] was the finding that reducing agents such as dithiothreitol and ascorbate could potentiate RNA cleavage by Fe(II)·BLM.

It has been shown previously that activation of Fe·BLM for DNA cleavage can be accomplished by the use of Fe(II)·BLM under aerobic conditions, or else by admixture of Fe(III)·BLM and H_2O_2.[14] As shown in Figure 4, activated Fe·BLM prepared in either fashion readily effected RNA strand scission when the tRNA^{His} precursor was used as a substrate. In spite of the fact that the activation of Fe(II)·BLM in the presence of peroxide was carried out at neutral pH, which is not optimal for producing DNA damage,[23] the extent of RNA cleavage was much greater than that achieved by admixture of Fe(II)·BLM + O_2 (Fig. 4, cf lanes 5 and 6). This may well reflect the need for a bimolecular collision of two Fe·BLM molecules to achieve activation in the aerobic system,[15] and possibly also the ability of DNA (and presumably RNA as well) to inhibit the aerobic activation of Fe(II)·BLM to which it has bound.[15b] The sites of cleavage of the tRNA^{His} precursor substrate were largely the same regardless of the mode of Fe·BLM activation, although at least one minor site of cleavage was uniquely associated with each activation method. Although this observation is believed to be reliable under the specific conditions employed for RNA cleavage in each system, it has not been investigated in sufficient detail to assess its possible mechanistic implications.

The actual chemistry of RNA degradation is relatively poorly defined at present. The observed dependence of RNA strand scission on ambient levels of oxygen (Fig. 3) is entirely consistent with observations made previously for DNA.[22] For DNA, there are two sets of products formed upon treatment with activated Fe·BLM. One of these affords frank strand scission, while the other affords an alkali labile lesion that can be 'unmasked' by subsequent treatment with reagents such as alkali or hydrazine.[3,7] While the nearly stoichiometric release of free uracil from tRNA^{His} concomitant with cleavage at U_{35} (Fig. 5) argues against the presence of a large proportion of an RNA-derived alkali labile lesion, subsequent treatment with hydrazine did produce a minor amount of a second product, consistent with the presence of an alkali labile lesion.

In this context, it may be noted that the formation of strand scission vs. alkali labile products in DNA is dependent on O_2 concentration.[24] At reduced oxygen concentrations, alkali labile lesions are formed due to the insufficiency of O_2 needed to react with the initially formed C4′ deoxyribose radical. In the case of RNA, no study has yet addressed the issue of the effect of O_2 concentration on the type and amounts of products formed. It is quite possible that an additional pathway for RNA degradation may become more readily apparent when O_2 is more limiting.

The functional groups present at the 3′-termini of the products shown in Figure 6 has not been established directly, but may be inferred from the results of two other types of experiments. Specifically, Fe(II)·BLM treatment of a 3′-^{32}P end labeled yeast ribosomal 5S RNA afforded oxidative degradation at U_{50}; the derived band on a polyacrylamide gel migrated faster than the analogous band resulting from treatment of the same RNA with a base-specific ribonuclease. The latter is known to contain a 5′-OH group, suggesting that the Fe·BLM-derived band terminated in a 5′-phosphate. When the same RNA was 5′-^{32}P end labeled, treatment

with Fe(II)·BLM again afforded a band that migrated faster than the analogous band resulting from treatment with a base-specific RNase, the latter of which has a 2′,3′-cyclic phosphate at its 3′-terminus. Thus the migration of the BLM-derived band is entirely consistent with the presence of an oligonucleotide 3′-phosphoroglycolate (Scheme 2).

Further evidence may be adduced from the experiment illustrated in Figure 8 and Table 2. Treatment of the chimeric octanucleotides C_3-*ribo*-CGCTAGCG and C_3-*ara*-CGCTAGCG with Fe(II)·BLM resulted in cleavage at the 3-position with concomitant formation of $CpGp_{CH_2COOH}$ (**1**) (Fig. 7). That the modified dinucleotide formed in this reaction actually had the assigned structure was based on the identical behavior of this material in comparison with an authentic synthetic sample when assayed by reverse phase HPLC (Table 2) and PAGE (Fig. 8). Also documented in Figure 8 is the appearance of new bands when Fe(II)·BLM-mediated C_3-*ara*-CGCTAGCC was subsequently treated with hydrazine. One of these comigrated with (5′-^{32}P end labeled) CpGp; another may well be the corresponding hydroxylated pyridazine derivative. This is entirely consistent with the effects observed when a DNA-derived alkaline-labile lesion was treated with hydrazine or an alkylamine.[7a] On the basis of these findings and the mobility of bands in the gel, it seems likely that the faster and slower migrating bands in lane 5 of Figure 6 have phosphoroglycolate and phosphate groups at their 3′-termini, respectively.

While there is no evidence for the involvement of C1′ H of DNA, or of the DNA strand of a DNA–RNA heteroduplex, in Fe(II)·BLM-mediated oligonucleotide degradation, the abstraction of this H atom from C_3-*ara* and C_3-*ribo*-CGCTAGCG by activated Fe·BLM seems highly likely, given the formation of the quinoxaline derivative of CpGp (**2**) upon subsequent treatment with 1,2-diaminobenzene (Scheme 4). Since the formation of this species has been documented carefully at qualitative and quantitative levels (Figs 8 and 9, Table 2) using the chimeric oligonucleotides as substrates, it is obviously important to determine whether it is also formed as a product of RNA degradation per se. As noted previously,[4g,16] the abstraction of C1′ H from the minor groove of RNA seems feasible based on the greater accessibility of C1′ H, as compared with C4′ H, within the wide, shallow groove of an A-form duplex.

Conclusions

Characterization of the nature of RNA degradation by Fe(II)·bleomycin indicates that RNAs generally exhibit the same features as substrates noted previously for DNA's. These include an increase in the extent of strand scission as the number of positively charged groups at the C-terminus of the BLM congener employed is increased. RNA cleavage requires oxygen and is facilitated by reducing agents. In common with DNA, bleomycin may be activated for RNA cleavage as a Fe(III) complex in the presence of H_2O_2. The chemistry of RNA cleavage appears to be initiated by abstraction of C4′ H and is likely to involve two sets of products analogous to those already established for DNA substrates. In addition, two chimeric DNA oligonucleotides having a single *ara* or *ribo* cytidine moiety at one site of cleavage afforded products whose formation can be rationalized readily only by initial abstraction of H from C1′ of the sugar moiety.

Experimental

Blenoxane was obtained from Bristol Laboratories and was fractionated to afford bleomycin A_2 and bleomycin demethyl A_2 as described.[25] BLM A_5 was a gift from Dr Li-He Zhang, Beijing Medical College. A pSP64 plasmid encoding *B. subtilis* $tRNA^{His}$ precursor flanked by an SP6 promotor and an *Eco* R1 restriction site was provided by Dr Barbara Vold, SRI International. *Eco* R1 restriction endonuclease and SP6 RNA polymerase were obtained from Boehringer Mannheim; RNasin ribonuclease inhibitor was from Promega. T4 polynucleotide kinase was purchased from United States Biochemical. $Fe(NH_4)_2SO_4$ was purchased from Alfa Products. QIAGEN columns were from QIAGEN. The radioisotopes employed ([γ-^{32}P]ATP (7000 Ci/mmol), [α-^{32}P]CTP (3000 Ci/mmol) and [5,6-^{3}H]UTP (43 Ci/mmol)) were obtained from ICN Radiochemicals.

5′-(4,4′-Dimethoxyytrityl)-*N*^{2}-isobutyryl-2′-deoxyguanosine-3′-[H-phosphono-(2″-*O*-hydroxyethyl)quinoxaline] (5). A mixture of 2-(2′-hydroxyethyl)quinoxaline (**4**)[26] (20 mg, 0.114 mmol) and 5′-DMTr-*N*^{2}-isobutyryl-2′-deoxyguanosine-3′-H-phosphonate (**3**) (112 mg, 0.14 mmol) were dried by repeated co-evaporation of portions of pyridine. The residue was dissolved in 5 mL of dry pyridine and treated with 43 μL (0.34 mmol) of trimethylacetyl chloride. The reaction mixture was stirred at room temperature for 1 h, then concentrated under diminished pressure to afford an oil. This oil was co-evaporated with portions of toluene to remove residual pyridine. The crude reaction mixture was purified by silica gel flash column chromatography (10 g column, packed with 1% CH_3OH in CH_2Cl_2). Elution with a stepwise gradient of 1%, 5% and then 8% CH_3OH in CH_2Cl_2 provided the product (**5**) as a pink film, yield 95 mg (80 %): silica gel TLC R_f 0.26 and 0.43 (8% CH_3OH in CH_2Cl_2); ^{1}H NMR ($CDCl_3$) δ (mixture of diastereomers) 1.01–1.25 (m, 6H), 2.23–2.50 (m, 2H), 2.80–2.96 (m, 1H), 3.04 (m, 2H), 3.39 (m, 2H), 3.73 (m, 6H), 4.06–4.19 (m, 3H), 4.65 (m, 2H), 5.46–5.66 (m, 1H), 5.94–6.08 (m, 1H), 6.73–7.28 (m, 13H), 7.34 (m, 2H), 7.71 (m, 1H), 7.96 (m, 2H) and 8.76 (m, 1H), mass spectrum (fast atom bombardment), *m/z* 860.316 $(M + 1)^+$ ($C_{45}H_{47}N_7O_9P$ requires 860.317).

***N*^{2}-Isobutyryl-2′-deoxyguanosine-3′-(H-phosphono-2″-(*O*-hydroxyethyl)quinoxaline) (6).** 5′-DMTr-protected **5** (110 mg, 0.13 mmol) was treated with 5 mL of a solution containing 0.5% (v/v) trifluoroacetic acid in $CHCl_3$ at 0 °C for 1 h, according to the procedure described by

Fujii et al.[27] The crude reaction mixture was concentrated and purified by silica gel flash chromatography (12 g column, packed with 1% CH_3OH in CH_2Cl_2). Elution with a stepwise gradient of 1%, 8%, then 20% CH_3OH in CH_2Cl_2 provided the product **6** as a colorless film, yield 38 mg (53%): silica gel TLC R_f 0.54 (20% CH_3OH in CH_2Cl_2); ^1H NMR ($CDCl_3$) δ 1.25 (m, 6H), 2.82 (m, 3H), 3.76–3.90 (m, 10H), 4.20 (m, 1H), 5.16–5.24 (m, 3H), 6.01 (m, 1H), 7.28 (m, 2H), 7.71 (m, 1H), 7.97 (m, 2H) and 8.78 (m, 1H).

5′-(4,4′-Dimethoxytrityl)-N^4-benzoyl-2′-deoxycytidylyl-(3′→5′)[N^2-isobutyryl-3′-(H-phosphono-2′-deoxyguanosine)]3′-[H-phosphono-2″-(*O*-hydroxyethyl)quinoxaline] (8). A mixture of alcohol **6** (37 mg, 66.4 μmol) and 5′-DMTr-N^4-benzoyl-2′-deoxycytidine-3′-H-phosphonate (**7**) (64 mg, 80.1 μmol) was dried by repeated coevaporation of portions of pyridine. The residue was dissolved in 3 mL of dry pyridine and the reaction was initiated by the addition of trimethylacetyl chloride (33 μL, 0.33 mmol). The reaction mixture was stirred at room temperature for 1 h, then concentrated under diminished pressure to afford an oil. This oil was coevaporated with portions of toluene to remove residual pyridine. The crude reaction mixture was purified by silica gel flash chromatography (20 g column, packed with 1% CH_3OH in CH_2Cl_2). Elution with a stepwise gradient of 1%, 8% and then 10% CH_3OH in CH_2Cl_2 provided the product (**8**) as a pink film, yield 32 mg (40%): silica gel TLC R_f 0.47 (10% CH_3OH in CH_2Cl_2); ^1H NMR ($CDCl_3$) δ (mixture of diastereomers) 1.06–1.22 (m, 6H), 2.31–2.80 (m, 4H), 3.10 (m, 1H), 3.30–3.39 (m, 4H), 3.77 (m, 6H), 4.33 (m, 3H), 4.70 (m, 3H), 5.02–5.55 (m, 2H), 6.02–6.22 (m, 2H), 6.81–7.74 (m, 25H), 7.93 (m, 1H) and 8.78 (m, 1H).

2′-Deoxycytidylyl-(3′→5′)[2′-deoxyguanosine-3′-(phosphoro-(2″-*O*-hydroxyethyl)quinoxaline)] (2). The fully protected H-phosphonate **8** (10 mg, 8.1 μmol) was oxidized using 2 mL of 0.1 M iodine in 7:2:1 tetrahydrofuran:pyridine:water. The reaction was quenched after 10 min by the addition of 1% aqueous $NaHSO_3$ and extracted with CH_2Cl_2. The CH_2Cl_2 layer was dried (Na_2SO_4) and concentrated under diminished pressure. The residue was dissolved in 6 mL of 3:1 NH_4OH:EtOH and heated at 40 °C for 12 h. The ammonia was removed under diminished pressure and the solution was acidified with glacial acetic acid. The reaction mixture was concentrated under diminished pressure. The crude mixture was purified by HPLC using a reverse phase C_8 column (10 × 250 mm); elution was effected with a linear gradient of 0.1 M aqueous ammonium acetate (pH 7.2) containing increasing amounts of acetonitrile (0–20 min, 0.1 M aqueous ammonium acetate; 20–22 min, a linear gradient from 0 to 6% CH_3CN in 0.1 M aqueous ammonium acetate; 32–50 min, 15% CH_3CN in 0.1 M aqueous ammonium acetate) at a flow rate of 3.0 mL/min. The product (**2**) eluted at 26.9 min and was isolated as a colorless solid, yield 1.1 mg (17%); mass spectrum (FAB), *m/z* 792 $(M + 1)^+$.

5′-^{32}P End labeled 2′-deoxycytidylyl(3′→5′)[2′-deoxyguanosine-3′-(phosphoro-2′-(*O*-hydroxyethyl)quinoxaline)]. A reaction mixture (20 μL total volume) containing 3.5 μg (4.5 nmol) of dinucleotide **2**, 167 μCi of [γ-^{32}P]ATP (7000 Ci/mmol), 10 mM $MgCl_2$, 100 μM spermidine, 100 μM EDTA and 10 units of T4 polynucleotide kinase in 50 mM Tris-HCl, pH 7.6, was incubated at 37 °C for 15 min. The reaction mixture was then treated with 2 μL of 5.8 mM ATP and incubated at 37 °C for an additional 15 min. The reaction mixture was purified by 20% denaturing polyacrylamide gel electrophoresis (17 watts) for 3 h. The gel was visualized by autoradiography. The radiolabeled band containing the product was excised from the gel and recovered by soaking in 2 M $LiClO_4$ at 25 °C for 30 min, then the product was recovered by precipitation and centrifugation.

5′-^{32}P End labeled oligonucleotides. The 5′-^{32}P end labeled $tRNA^{His}$ precursor transcript was prepared as described.[4e] Oligonucleotides CGCTAGCG, C_3-*ribo*-CGCTAGCG and C_3-*ara*-CGCTAGCG were prepared as described.[16] Each was radiolabeled by dissolving ~1 μg of the oligomer in 25 μL of 50 mM Tris-HCl, pH 7.6, containing 10 mM $MgCl_2$, 100 μM spermidine, 100 μM EDTA, 0.17 mCi of [γ-^{32}P]ATP and 30 units of T4 polynucleotide kinase. The reaction mixture was incubated at 37 °C for 2 h and the end labeled octanucleotides were purified by 20% polyacrylamide gel electrophoresis.

Fe·BLM-mediated degradation of $tRNA^{His}$ precursor. Typical reaction mixtures (5 μL total volume) contained approximately 0.5–5.0 μM labeled RNA in 5 mM Na phosphate, pH 7.5. The reactions were initiated by the simultaneous addition of Fe^{2+} and BLM to the concentrations indicated in the figure legends and incubated at 22 °C for 15 min. The reactions were analyzed by polyacrylamide gel electrophoresis. Reactions designed to determine the effects of reducing agents were carried out in the same fashion, but in the presence of the indicated amount of reductant.

Treatment with hydrazine. Following incubation with Fe(II)·BLM, the cleavage reaction (5 μL total volume) was treated with 50 mM hydrazine (NH_2NH_2·HCl, pH 8) and 4 mM EDTA (final concentrations). The combined reaction mixture was incubated at 0 °C for 15 min. Hydrazine was removed by lyophilization prior to polyacrylamide gel electrophoretic analysis.

Treatment with NaOH. Following incubation with Fe(II)·BLM, the cleavage reaction was treated with 0.2 N NaOH and 2 mM EDTA (final concentrations) at 90 °C for 3 min. The reaction was stopped on dry ice and neutralized with 1 equiv of hydrochloric acid prior to polyacrylamide gel electrophoretic analysis.

Effect of oxygen concentration on Fe·BLM-mediated $tRNA^{His}$ precursor degradation. Prior to use, all reaction components were lyophilized to dryness and stored at −80 °C. Water used in the experiment was

alternately purged under vacuum and saturated with N_2, then stored under anaerobic conditions. All reactions were performed in a dry box under reduced oxygen conditions of approximately 3–4 ppm. All components (except H_2O) were subjected to vacuum immediately prior to performing the reaction. Reaction components were dissolved in deoxygenated water under reduced oxygen conditions immediately prior to the reaction; Fe^{2+} was dissolved immediately prior to initiation of the reaction.

Reaction mixtures (5 μL total volume) contained approximately 3 μM 5′-^{32}P end labeled precursor $tRNA^{His}$ (final nucleotide concentration) and equal concentrations of Fe^{2+} and BLM in 5 mM NaH_2PO_4, pH 7.0. Reaction mixtures were incubated at 22 °C for 15 min, quenched by the addition of 5 mM EDTA and incubated for an additional 10 min. The reactions were then analyzed by denaturing polyacrylamide gel electrophoresis under ambient oxygen conditions.

Cleavage of $tRNA^{His}$ precursor transcript by Fe(III)·BLM + H_2O_2. Reaction mixtures (5 μL total volume) contained approximately 3 μM 5′-^{32}P end labeled precursor $tRNA^{His}$ (final nucleotide concentration) and equal concentrations of Fe^{3+} and BLM in 5 mM NaH_2PO_4, pH 7.0. Hydrogen peroxide was added to initiate the reaction approximately 30 s after preincubation of Fe(III)·BLM A_2 in the presence of the RNA substrate. Reactions were incubated at 22 °C for 15 min and analyzed by electrophoresis on 10% denaturing polyacrylamide gels.

Quantification of products formed concomitant with cleavage of $tRNA^{His}$ precursor at uridine$_{35}$. Transcriptional incorporation of [5,6-^{3}H]UTP and [α-^{32}P]CTP into $tRNA^{His}$ precursor was accomplished from an *Eco* R1-linearized pSP64 plasmid encoding *B. subtilis* $tRNA^{His}$ precursor. The desired RNA product was transcribed in a reaction mixture (50 μL total volume) containing 40 mM Tris–HCl, pH 7.9, 6 mM $MgCl_2$, 2 mM spermidine, 10 mM dithiothreitol, 4 units of RNasin (1 unit inhibits by 50% the activity of 5 ng of ribonuclease A), 0.5 mM ATP, CTP and GTP, 0.44 mM UTP, 40 μCi [α-^{32}P]CTP, 100 μCi [5,6-^{3}H]UTP, 66 units of SP6 RNA polymerase (one unit incorporates 1 nmol of ribonucleotide into acid-precipitable material in 1 h at 37 °C) and 2.3 μg of linearized plasmid DNA. The reaction was incubated at 37 °C overnight and purified on a QIAGEN-tip 5 column. The purified RNA was then used in the following Fe(II)·BLM cleavage reactions.

Reactions (either 500 μL or 100 μL total volume) contained 5 mM Na phosphate, pH 7.5, 1.4 μg of $tRNA^{His}$ precursor and the indicated concentrations of Fe^{2+} and BLM. Final RNA nucleotide concentration in the 500 μL reactions was 8.5 μM and in the 100 μL reactions was 42.5 μM. The reaction was initiated by the simultaneous addition of Fe^{2+} and BLM and incubated at 22 °C for 15 min. An aliquot of the reaction mixture (representing 4% of the total volume) was then removed, dried and subsequently analyzed by denaturing 20% polyacrylamide gel electrophoresis to permit quantification of the extent of cleavage of the $tRNA^{His}$ precursor substrate.

Analysis of the cleavage reaction by HPLC. The remaining reaction mixture was dried and redissolved in 25 μL of water; a portion (23 μL) was analyzed by HPLC (Alltech C_{18} Lichrosorb column; 0.1 M NH_4OAc mobile phase; detection at 260 nm). Fractions were collected every 30 (or 10) s, quantitated by scintillation counting and the elution time of the radioactive peak was compared with retention times of known standards (e.g., uracil).

Cleavage of octanucleotides by Fe(II)·BLM for PAGE analysis. Reaction mixtures (5 μL total volume) contained 6.25 μM octanucleotide (50 μM nucleotide concentration) in 10 mM sodium cacodylate, pH 7.0. Reactions containing BLM A_2 at the indicated concentrations were initiated by the addition of Fe^{2+} and incubated at 0 °C for 35 min. Where indicated, the incubation was followed by treatment of the reaction mixture with 5 μL of 1:1 EtOH:H_2O containing 0.5 M 1,2-diaminobenzene for 30 min at 55 °C. The cooled solution was extracted with ether and concentrated prior to analysis. In reactions treated with hydrazine, 5 μL of 0.5 M aqueous hydrazine (pH 8.0) was added to the reaction mixture subsequent to Fe·BLM treatment; the reaction mixture was incubated at 0 °C for 20 min. The excess hydrazine was then removed under diminished pressure. Analysis was carried out by 20% denaturing polyacrylamide gel electrophoresis.

Cleavage of octanucleotides by Fe(II)·BLM for HPLC analysis. Reaction mixtures (50 μL total volume) contained 250 μM octanucleotide (2 mM final nucleotide concentration), 0.4 mM BLM A_2 and 0.8 mM Fe^{2+} in 100 mM sodium cacodylate, pH 7.0. Reactions were saturated with oxygen (O_2 bubbling) and initiated by the addition of Fe^{2+}. Reaction mixtures were incubated at 0 °C for 35 min. An aliquot (25 μL) of each reaction was then removed and analyzed by HPLC on a C_{18} column (3 μm) using an isocratic flow rate of 0.1 M aqueous ammonium acetate (pH 7.0) at a flow rate of 1.4 mL/min. Reaction products were determined and quantitated based on comparison of HPLC elution times and peak areas with those authentic samples.[10,16,17]

An aliquot of the reaction (25 μL) was subsequently treated with 25 μL of 1:1 ethanol:water (v/v) containing 0.5 M 1,2-diaminobenzene. The combined solution was heated at 55 °C for 30 min. The cooled solution was extracted with ether and concentrated prior to HPLC analysis on a C_{18} reverse-phase column. The column was washed with a linear gradient of 0.1 M aqueous ammonium acetate (pH 7.2) containing increasing amounts of CH_3CN (0–20 min, 0.1 M aqueous ammonium acetate; 22–32 min, a linear gradient from 0 to 6% CH_3CN in 0.1 M aqueous ammonium acetate; 32–50 min, 15% CH_3CN in 0.1 M aqueous ammonium acetate) at a flow rate of 1.4 mL/min. The eluate was

monitored at 260 and 320 nm. When detected, the peak at 33.9 min coeluted with an authentic quinoxaline-derivatized dinucleotide standard. Yields were corrected for decomposition, which had been determined using the authentic standard under the conditions of the BLM reaction.

The HPLC-purified product was 5′-^{32}P end labeled as described above for synthetic dinucleotide **2**.

Acknowledgement

This work was supported by NIH research grant CA53913 from the National Cancer Institute.

References

1. (a) Umezawa, H. In: *Bleomycin: Current Status and New Developments*; Carter, S. K.; Crooke, S. T.; Umezawa, H., Eds.; Academic; New York, 1978; pp 15–20; (b) Sugiura, Y.; Takita, T.; Umezawa, H. *Met. Ions Biol. Syst.* **1985**, *19*, 81.

2. (a) Tanaka, W. *J. Antibiot.* **1977**, *30*, S41; (b) Hecht, S. M. In *Cancer Chemotherapeutic Agents*, p 369, Foye, W. O., Ed.; American Chemical Society: Washington, DC, 1995.

3. (a) Hecht, S. M. *Acc. Chem. Res.* **1986**, *19*, 383; (b) Stubbe, J.; Kozarich, J. W. *Chem. Rev.* **1987**, *87*, 1107; (c) Natrajan, A.; Hecht, S. M. In: *Molecular Aspects of Anticancer Drug-DNA Interactions*; Neidle, S.; Waring, M., Eds.; Macmillan: London, 1993; p 197; (d) Kane, S. A.; Hecht, S. M. *Prog. Nucleic Acid Res. Mol. Biol.* **1994**, *49*, 313.

4. (a) Magliozzo, R. S.; Peisach, J.; Ciriolo, M. R. *Mol. Pharmacol.* **1989**, *35*, 428; (b) Carter, B. J.; de Vroom, E.; Long, E. C.; van der Marel, G. A.; van Boom, J. H.; Hecht, S. M. *Proc. Natl. Acad. Sci. U.S.A.* **1990**, *87*, 9373; (c) Carter, B. J.; Reddy, K. S.; Hecht, S. M. *Tetrahedron* **1991**, *47*, 2463; (d) Hüttenhofer, A.; Hudson, S.; Noller, H. F.; Mascharak, P. K. *J. Biol. Chem.* **1992**, *267*, 24471; (e) Holmes, C. E.; Carter, B. J.; Hecht, S. M. *Biochemistry* **1993**, *32*, 4293; (f) Dix, D. J.; Lin, P.-N.; McKenzie, A. R.; Walden, W. E.; Theil, E. C. *J. Mol. Biol.* **1993**, *231*, 230; (g) Hecht, S. M. *Bioconjugate Chem.* **1994**, *5*, 513.

5. Morgan, M. A.; Hecht, S. M. *Biochemistry* **1994**, *33*, 10286.

6. (a) D'Andrea, A. D.; Haseltine, W. A. *Proc. Natl. Acad. Sci. U.S.A.* **1978**, *75*, 3608; (b) Takeshita, M.; Grollman, A. P.; Ohtsubo, E.; Ohtsubo, H. *Proc. Natl. Acad. Sci. U.S.A.* **1978**, *75*, 5983; (c) Mirabelli, C. K.; Ting, A.; Huang, C.-H.; Mong, S.; Crooke, S. T. *Cancer Res.* **1982**, *42*, 2779.

7. (a) Sugiyama, H.; Xu, C.; Murugesan, N.; Hecht, S. M. *J. Am. Chem. Soc.* **1985**, *107*, 4104; (b) Rabow, L. E.; Stubbe, J.; Kozarich, W.; Gerlt, J. A. *J. Am. Chem. Soc.* **1986**, *108*, 7130; (c) Sugiyama, H.; Xu, C.; Murugesan, N.; Hecht, S. M.; van der Marel, G. A.; van Boom, J. H. *Biochemistry* **1988**, *27*, 58.

8. Green, C. J.; Vold, B. S. *J. Biol. Chem.* **1988**, *263*, 652.

9. Caruthers, M. H. *Science* **1985**, *230*, 281.

10. (a) Sugiyama, H.; Kilkuskie, R. E.; Hecht, S. M. *J. Am. Chem. Soc.* **1985**, *107*, 7765; (b) Sugiyama, H.; Kilkuskie, R. E.; Chang, L.-H., Ma, L.-T.; Hecht, S. M.; van der Marel, G. A.; van Boom, J. H. *J. Am. Chem. Soc.* **1986**, *108*, 3852.

11. (a) Takeda, K., Kato, F.; Kawai, S.; Kono, K. *J. Antibiot.* **1979**, *32*, 43; (b) Berry, D. E.; Chang, L.-H.; Hecht, S. M. *Biochemistry* **1985**, *24*, 3207.

12. Kross, J.; Henner, W. D.; Hecht, S. M. Haseltine, W. A. *Biochemistry* **1982**, *21*, 3711.

13. See, however, (a) Gajewski, E.; Aruoma, O. I.; Dizdaroglu, M.; Halliwell, B. *Biochemistry* **1991**, *30*, 2444; (b) Chakrabarti, S.; Makrigiorgos, G. M.; O'Brien, K.; Bump, E.; Kassis, A. I. *Free Radic. Biol. Med.* **1996**, *20*, 777.

14. Burger, R. M.; Peisach, J.; Horwitz, S. B. *J. Biol. Chem.* **1981**, *256*, 11636.

15. (a) Kuramochi, H.; Takahashi, K.; Takita, T.; Umezawa, H. *J. Antibiot.* **1981**, *34*, 576; (b) Van Atta, R. B.; Long, E. C.; Hecht, S. M.; van der Marel, G. A.; van Boom, J. H. *J. Am. Chem. Soc.* **1989**, *111*, 2722.

16. Duff, R. J.; de Vroom, E.; Geluk, A.; Hecht, S. M.; van der Marel, G. A.; van Boom, J. H. *J. Am. Chem. Soc.* **1993**, *115*, 3350.

17. Murugesan, N.; Xu, C.; Ehrenfeld, G. M.; Sugiyama, H.; Kilkuskie, R. E.; Rodriguez, L. O.; Chang, L.-H.; Hecht, S. M. *Biochemistry* **1985**, *24*, 5735.

18. It may be noted from Table 2 that the amount of cytosine propenal formed from C_3-*ara*-CGCTAGCG in this experiment was significantly in excess of the amount of 5′-GMP. This finding did not obtain in other experiments with the same substrate.

19. Duff, R. J. Ph.D. thesis, University of Virginia, 1994.

20. Levy, M. J.; Hecht, S. M. *Biochemistry* **1988**, *27*, 2647.

21. Holmes, C. E.; Hecht, S. M. *J. Biol. Chem.* **1993**, *268*, 25909.

22. Sausville, E. A.; Stein, R. W.; Peisach, J.; Horwitz, S. B. *Biochemistry* **1978**, *17*, 2746.

23. Natrajan, A.; Hecht, S. M.; van der Marel, G. A.; van Boom, J. H. *J. Am. Chem. Soc.* **1990**, *112*, 3997.

24. (a) Burger, R. M.; Peisach, J.; Horwitz, S. B. *J. Biol. Chem.* **1982**, *257*, 3372; (b) Burger, R. M.; Peisach, J.; Horwitz, S. B. *J. Biol. Chem.* **1982**, *257*, 8612; (c) Wu, J. C.; Kozarich, J. W.; Stubbe, J. *J. Biol. Chem.* **1983**, *258*, 4694; (d) Wu, J. C.; Kozarich, J. W.; Stubbe, J. *Biochemistry* **1985**, *24*, 7652.

25. Chien, M.; Grollman, A. P.; Horwitz, S. B. *Biochemistry* **1977**, *16*, 3641.

26. Elina, A. S.; Tsyrul'nikova, L. G. *Zh. Obshch. Khim.* **1964**, *34*, 2077.

27. Fujii, M.; Ozaki, K.; Kume, A.; Sekine, M.; Hata, T. *Tetrahedron Lett.* **1986**, *27*, 935.

(*Received in U.S.A.* 15 *October* 1996; *accepted* 19 *December* 1996)